Spectral, thermal and structural studies on aluminium phthalocyanine hydroxide thin films

SUSAN MATHEW[*], C. SUDARSANAKUMAR[a], C. S. MENON[a]
Department of Physics, St.Thomas College, Kozhencherry, Pathanamthitta , Kerala, India
[a]*School of Pure and Applied Physics, Mahatma Gandhi University, Kottayam Kerala, India*

Vacuum evaporated thin films of aluminium phthalocyanine hydroxide were prepared at room temperature onto glass substrates at a base pressure of 10^{-5} torr. Annealing was done in air and the effect of annealing temperature on the electrical, optical and structural properties were studied. Arrhenius plot yields thermal activation energy in the intrinsic region and impurity scattering region. Optical absorption spectra of films annealed at temperatures 348 K, 398 K and 448 K were taken over a wavelength range of 350 to 900 nm and the optical energy band gap E_g and the onset energy gap were calculated. Refractive index n, extinction coefficient k and the real and imaginary parts of the optical dielectric constant ε_1 and ε_2 were also evaluated and were plotted against the photon energy. Photoluminescence (PL) spectrum was investigated to identify impurity levels and to gauge disorder and interface roughness. Scanning electron microscope (SEM) images were taken to study the surface morphology of the film. X-ray diffraction pattern was used to find the nano-crystalline grain size using Scherrer formula. An increase in grain size with annealing temperature was observed.

(Received January 03, 2009; accepted Janaury 19, 2010)

Keywords : Thin film, Activation energy, Refractive index, Optical band gap

1. Introduction

In the past two decades organic thin film technology and its device applications have attracted the interest of researchers and industry due to their interesting optoelectronic properties [1]. Because of their attractive processing characteristics and demonstrated performance, organic semiconductors could compliment or even replace silicon-based technology for existing or emerging thin film transistor applications requiring large area coverage, structural flexibility and low temperature processing. Their application in new flexible and transparent devices [2,3] and their tuning possibilities lead to an increase of the academic activity in this field. They are promising materials for development of various modern and future technologies in solid-state devices such as field-effect transistors, light emitting diodes, optical recording, organic solar cells and sensors [4-11]. Electronic charge transport in organic molecules does not require perfect single crystals. A regular arrangement of atoms, ions or molecules over a distance of only a few lattice spacing of the structural units is necessary for the electronic charge transport and is usually a sufficient condition for electrical conductivity of the organic system. Knowledge of the molecular structure and semiconducting characteristics of the organic compounds, allows the design of new materials that have pre-defined and controlled characteristics.

Though there are a large number of organic semiconducting materials, phthalocyanines are getting more attention due to their high thermal and chemical stability. They can be easily crystallized and sublimed, resulting in materials of purity 10^{14}–10^{16} traps / cm^3, which is rare in molecular chemistry. Metallophthalocyanines (PcMs) undergo no noticeable degradation up to 400-500^{0}C in air and in vacuum most complexes do not decompose below 900 °C [12]. PcMs show a number of special properties, such as electrical, optical and opto-electronic, which account for the great interest they have always aroused. The versatility, architectural flexibility and low cost of preparation make them eligible candidates for the fabrication of thin-film electronic molecular devices such as photovoltaic devices [13], photodetectors [14], organic transistors [15], organic electroluminescence devices [16] and sensors [17]. In recent years, they have received particular attention in the field of optical limiting for the development of highly efficient optical power protectors for sensitive optical instruments [18]. They are also promising candidates for medical applications because they show a strong Q-band in the absorption spectrum, located in the red region in which the tissue is rather transparent and they are fluorescent, which provides an opportunity for the establishment of their localization in the tissue. Therefore, they have already been widely investigated in view of their possible applications in photodynamic therapy and photodynamic diagnosis. It is observed that the electrical, optical and structural properties of PcM thin films are dependent on various parameters such as evaporation rate, thickness of the film and post-deposition annealing. In the present work we study the electrical, optical and structural properties of AlPcOH thin films annealed at various temperatures. Among the various metallophthalocyanine derivatives, trivalent aluminium phthalocyanine hydroxide is of great interest for its use as a toner in an electro-photographic developer. It is now utilized in a wide variety of fields such as solar cells and clinical photodynamic

therapy. The molecular structure of AlPcOH ($C_{32}H_{17}AlN_8O$) is shown in Fig. 1.

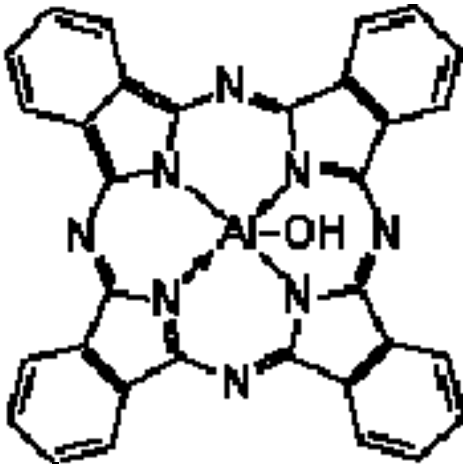

Fig. 1. The molecular structure of AlPcOH.

2. Experimental details

Aluminium phthalocyanine hydroxide powder procured from Aldrich, USA was evaporated in vacuum using a Hind Hivac 12A coating unit onto well cleaned microglass slides held at a pressure of 10^{-5} torr. Thin films were prepared by resistive heating of the powder from a molybdenum boat and the evaporation rate was kept constant as 10-12 nm/min. Several films of same thickness were prepared in the same experimental condition simultaneously. The reproducibility of the result was confirmed by making several such depositions under the same deposition conditions. Thickness of the film was determined by Tolansky's multiple beam interference technique [19].

AlPcOH thin films of thickness 335±5 nm were annealed in air for 1 hour at temperatures 348 K, 398 K and 448 K in a furnace whose temperature could be controlled by a controller cum recorder. UV- Visible absorption spectra were recorded using a Shimadzu 160 A UV –Visible spectro-photometer. The absorption edge was analyzed to get the optical band gap of AlPcOH. For electrical conductivity studies evaporated silver was used as the contact electrode. Thin copper strands were fixed by silver paste and the film was placed onto a hollow copper block in the conductivity cell, which was heated. The temperature of the sample was measured using Chromel-Alumel thermocouple. The electrical conductivity studies were done in the temperature range 330-525K. The resistance was noted at regular intervals of 5K using a programmable Keithley electrometer (Model No 617). The change of conductivity during cooling of the sample from 525 -330 K was also studied. To avoid any possible contamination, measurements were performed in vacuum at 10^{-3} Torr.

3. Results and discussion

3.1 Optical studies

The optical absorption spectrum of the film annealed in air at 448 K over a wavelength range of 350-900 nm is shown in Fig. 2.

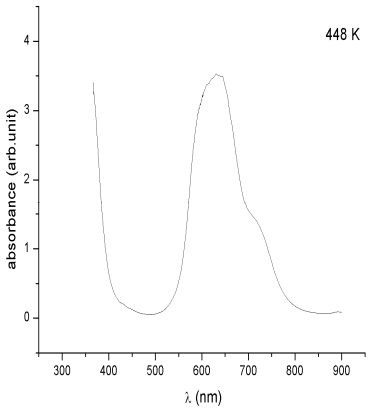

Fig. 2. The optical absorption spectrum of the film annealed in air at 448 K.

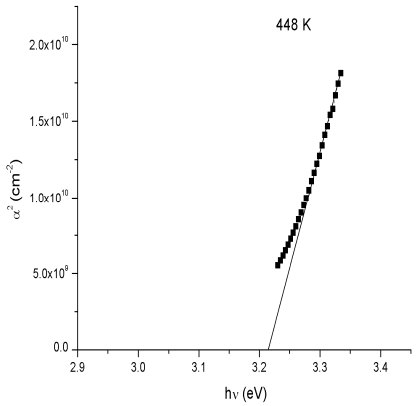

Fig. 3. Plot of α^2 versus $h\nu$ for the film annealed at 448 K.

In the case of AlPcOH thin films the two well-defined absorption bands of the phthalocyanine molecules namely B band and Q band were observed. The spectrum of phthalocyanine is believed to originate from orbitals within the aromatic 18π electron system and from overlapping orbitals on the central metal atom [20]. The π and π^* molecular orbitals are the highest occupied molecular orbital (HOMO) and the lowest unoccupied molecular orbital (LUMO) respectively in terms of molecular physics. In phthalocyanines the direct electronic transition from π to π^* orbitals in the energy range 300-450 nm results in an intense band called B-band (Soret band) which corresponds to the fundamental absorption from which the energy band gap is obtained [21]. The Q-band appeared in the 600-800 nm range gives onset energy [22]. The fundamental absorption edge was analyzed within the one electron theory of Bardeen [23] to

obtain information about direct or indirect interband transitions. The absorption coefficient α was calculated using the relation

$$\alpha = 2.303\ A/t \quad (1)$$

where A is the absorbance of the film and t is its thickness. For direct allowed transition, the absorption coefficient α is related to the photon energy hν by the relation

$$\alpha = \alpha_o\ (h\nu - E_g)^{1/2} \quad (2)$$

where Eg is the optical band gap and α_o a constant. A satisfactory straight line fit is obtained for α^2 as a function of hν, showing the existence of a direct band gap. The value of absorption coefficient α greater than 10^4 cm^{-1} obtained is also related to direct inter-band transitions. By plotting α^2 versus hν and extrapolating to zero absorption, the band gap Eg is obtained. Plot of α^2 versus hν for the film annealed at 448 K is shown in Fig.3. The values of fundamental and onset energy gaps are determined from the graph and are given in Table 1. The results showed no effect of the annealing temperature on the optical properties and hence the stability of the structure of AlPcOH thin film.

Table 1. Optical band gap, onset energy gap and grain size of AlPcOH thin films annealed at different temperatures.

Annealing temperature K	Optical band gap eV	Onset energy gap eV	Grain size nm
348	3.21	1.63	34.93
398	3.22	1.62	38.65
448	3.22	1.62	45.76

The reflectance spectrum of AlPcOH thin film is given in Fig. 4.

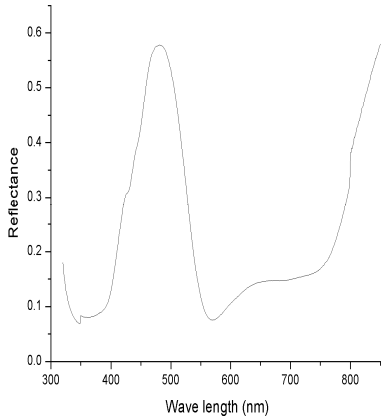

Fig. 4. The reflectance spectrum of AlPcOH thin film.

The main feature of the reflection spectrum is the sharp rise in reflectivity at ~ 500 nm. The optical properties of any material are characterized by two parameters the extinction coefficient k and the refractive index n. The extinction coefficient is calculated using Eq. (3) and n, using Eq. (4).

$$k = \frac{\alpha\lambda}{4\pi} \quad (3)$$

$$R = \frac{(n-1)^2 + k^2}{(n+1)^2 + k^2} \quad (4)$$

Fig. 5 shows the variation of refractive index n and extinction coefficient k with photon energy for AlPcOH thin film. For AlPcOH thin film of thickness 335 nm the maximum value of refractive index is 7.32 at 2.57 eV. Similar result is reported by Senthilarasu *et al.* [24] for zinc phthalocyanine thin films. The refractive index and the extinction coefficient are used for the calculation of the real and imaginary parts of the dielectric constant. The real and imaginary parts of the dielectric constant ε_1 and ε_2 are calculated using the expressions [25]

$$\varepsilon_1 = n^2 - k^2 \quad (5)$$

$$\varepsilon_2 = 2nk \quad (6)$$

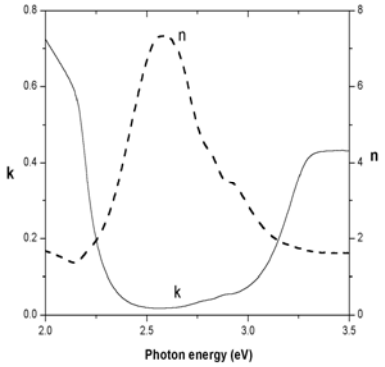

Fig. 5. Variation of n and k with photon energy for AlPcOH thin film.

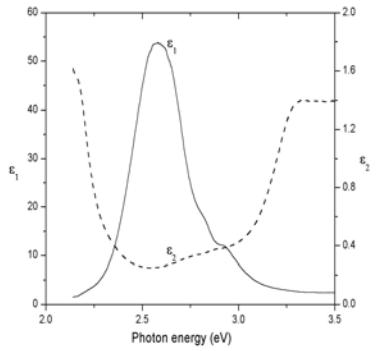

Fig. 6. Variation of ε_1 and ε_2 with photon energy for AlPcOH thin film.

Fig. 6 shows the variation of ε_1 and ε_2 with photon energy for AlPcOH thin film. The real part ε_1 is related to dispersion, while the imaginary part ε_2 provides a measure of the dissipation rate of the wave in the material. The real part ε_1 showed maximum value at 2.57 eV for AlPcOH thin film. A similar behaviour has been observed for chloroaluminium phthalocyanine thin films [26].

3.2 Photoluminescence study

Photoluminescence (PL) spectroscopy is a selective and extremely sensitive probe of discrete electronic states. The PL spectrum provides the transition energies, which can be used to determine electronic energy levels. Features of the emission spectrum can be used to identify surface, interface and impurity levels. The intensity of the PL signal provides information on the quality of surfaces and interfaces. It also gives a measure of the relative rates of radiative and nonradiative recombination.

The excitation energy and optical intensity can be chosen to study different regions and recombination mechanisms near interfaces. Since absorption of the incident light depends on the excitation energy, this parameter determines the depth of the PL probe. The excitation intensity is even more important, controlling the density of photoexcited electrons. This density is critical in the interpretation of recombination dynamics. The PL emission efficiency is determined by the ratio of radiative and nonradiative transitions. The nonradiative transition is induced by crystal imperfections such as point defects, dislocations and grain boundaries. Generally, direct band gap semiconductors have two emission peaks, a near band edge emission (NBE ~3.14 eV) and a deep level emission (DLE) at higher wavelength (~2.2 eV) [27, 28]. The NBE emission is due to excitons, while intrinsic and extrinsic defects contribute to DLE [29, 30]. High crystallinity is one of the most important factors in achieving a better NBE to DLE ratio. PL spectrum of the annealed sample was recorded at room temperature using 325 nm line (this corresponds to the excitation in the range of the Soret band) of a He : Cd laser as an excitation source. The photoluminescence spectrum of AlPcOH film is depicted in Fig. 7.

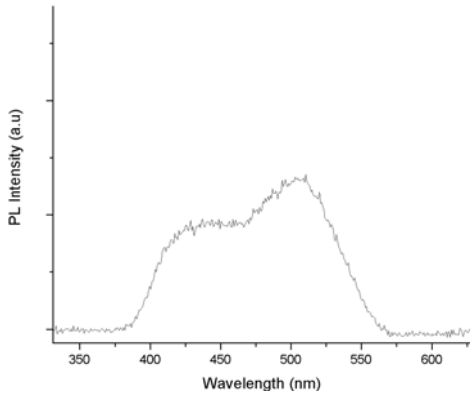

Fig. 7. Photoluminescence spectrum of AlPcOH thin film.

For AlPcOH film, the peaks were observed at 443 nm (2.80eV) and 504 nm (2.46 eV). These emissions are below the optical band gap (3.22 eV) and this indicates the presence of defects in the film. The PL intensity of the deep level green emission at 504 nm is greater in AlPcOH thin films. When the film is annealed at high temperature in air, the adsorbed oxygen and other defects such as vacancies, grain boundaries and dislocations are not removed completely and the corresponding impurity and defect levels are present in the band gap. So the film becomes more non-stoichiometric and the emission intensity from these deep levels increases.

3.3 Electrical studies

Semiconducting properties of phthalocyanines were first observed by Eley [31]. The electrical conductivity σ of a film of resistance R, length l, breadth b and thickness t is given by

$$\sigma = l/Rbt \tag{7}$$

The electrical conductivity can also be expressed as

$$\sigma = \sigma_0 \exp(-E/k_BT) \tag{8}$$

where σ is the conductivity at temperature T, E is the thermal activation energy, k_B is the Boltzmann constant and σo is the pre-exponential factor. The graphs of ln σ vs. 1000/T for air annealed films are shown in Fig. 8.

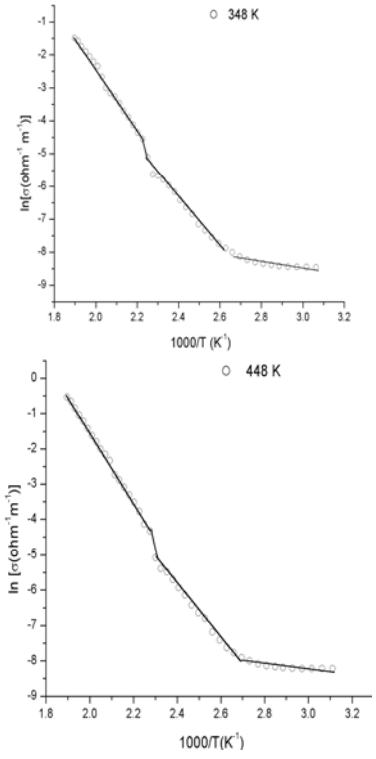

Fig. 8. Graph of ln σ vs. 1000/T for AlPcOH films annealed at 348 K and 448 K.

Each curve has three different slopes in the lower and higher temperature regions. From the slopes of these graphs activation energies are evaluated and collected in Table 2.

Table 2. Variation of activation energy with annealing temperature.

Annealing temperature (K)	Activation energy		
	E1	E2	E3
348	0.83	0.64	0.06
398	0.86	0. 66	0.05
448	0.87	0.68	0.05

The activation energy is determined within an accuracy of ±0.01 eV in all measurements. As shown by Belgachi and Collins [32], activation energy obtained may be interpreted as the difference between dominant energy levels. There are three linear regions for each graph, which correspond to three activation energies E_1, E_2 and E_3. The activation energy E_1 corresponding to the higher temperature region is associated with the resonant energy involved in a short lived excited state and E_2 and E_3 are associated with a short lived charge transfer between impurity and the complex [33]. In the low temperature range conductivity is due to hopping of charge carriers between the neighbours in the localized states near the Fermi level. As temperature increases activation energy also increases. The change in the slope and hence the activation energy is interpreted as a change from extrinsic to intrinsic conduction. Activation energy increases with increase in annealing temperature. In the case of phthalocyanines, oxygen is bound much more tenaciously. The role of adsorbed oxygen is to create carriers and to act as impurity in the extrinsic conduction region. Heat treatment in air does not remove oxygen completely. The removal of oxygen causes redistribution of traps and hence activation energy changes with annealing temperature. The conduction process in AlPcOH is found to be controlled by different trap levels present in the forbidden energy gap.

3.4 Structural studies

Fig. 9 shows the X-ray diffraction patterns of AlPcOH thin films annealed in air at 348 K and 448 K.

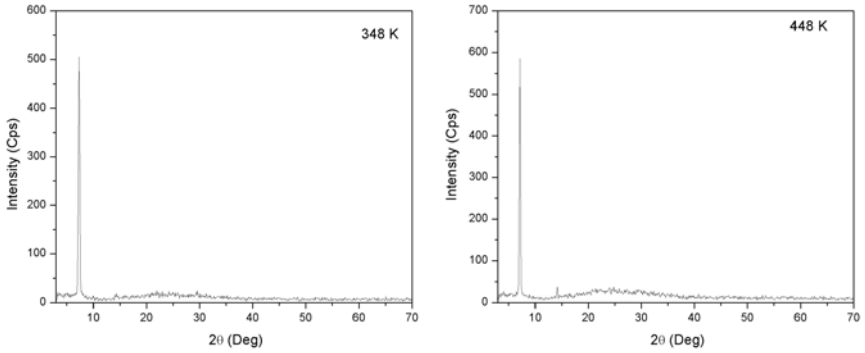

Fig. 9. X-ray diffraction patterns of AlPcOH thin films annealed in air at 348 K and 448 K

The grain size L of the film was calculated using the Scherrer formula [34]

$$L = K\lambda / b \cos\theta \quad (9)$$

where λ is the wave length of the X–ray beam (λ =0.15425 nm of Cu Kα1), b is the value of the full width at half maximum (FWHM) of the most intense peak, θ is the corresponding Bragg angle and K is Scherrer constant. The value of K, in general, depends on the crystallite shape and it is assigned a value of 0.9 for phthalocyanine films [35]. The grain sizes of AlPcOH thin films annealed at different temperatures are given in Table 1.

It is observed that the grain size increases as the annealing temperature increases from 348 to 448 K and a grain size of 45.76 nm is obtained for AlPcOH thin film annealed at 448 K. The increase in the grain size suggests a higher degree of crystallinity due to annealing. This increased crystallinity is attributed to the destruction of pseudomorphic layers, created in the film during formation.

The scanning electron micrographs shown in Fig. 10 display the development of the surface morphology of AlPcOH films with increasing annealing temperature.

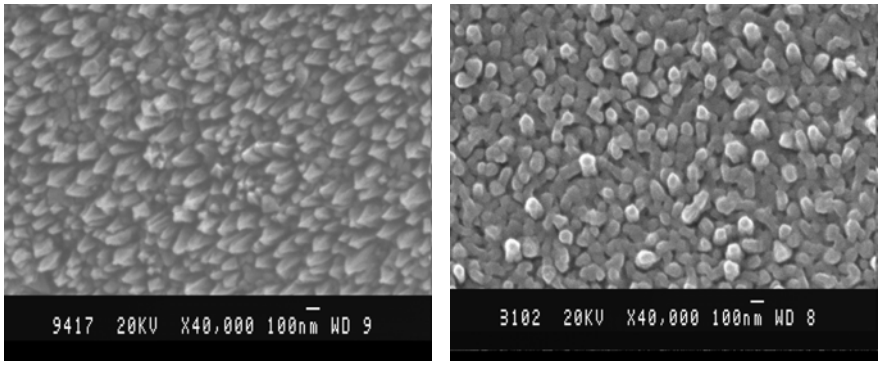

Fig. 10. Scanning electron micrographs of AlPcOH films annealed at 348 K and 448K.

It provides a pictorial display of the surface layer with a high depth of focus and thus providing better details of the surface. From the SEM planar view, it is clear that the film is made of homogeneous small crystal grains with grain size in the range 40-100 nm.

4. Conclusions

The absorption spectra of AlPcOH thin films show two absorption bands which we have identified as the fundamental absorption at high energies (B-band) and the exciton absorption at low energies (Q- band). From the XRD analysis it is seen that the grain size increases as the annealing temperature increases from 348-448 K. However, it is noticed that the band gap does not show much variation with the grain size which corresponds to various annealing temperatures. This is because the crystallite size is not small enough to show a distinct variation of the band gap. The activation energy is calculated from the electrical conductivity studies. There are three activation energies, which are due to the intrinsic charge carriers (E_1) and the impurity scatterings (E_2 and E_3). Thermal annealing treatment for a sufficiently long period of time may cause migration or diffusion of some atoms leading to a stable phase and films with improved polycrystalline structure and large grain size. The films show a higher conductance than the normal amorphous films.

References

[1] C. W.Tang, Appl.Phys.Lett. **48,** 183 (1986).
[2] C. D. Dimitrakopoulos, P. R. L.Malenfant, Adv. Mater**. 14**, 99 (2002).
[3] H. Y.Choi, S. H. Kim, J. Jang, Adv.Mater**. 16,** 732 (2004).
[4] W. E.Howard, O. F. Prache,IBM J. Res. and Dev. **45**(1), 115 (2001).
[5] D. Hohnholz, S. Steinbrecher, M. Hanack, J. Mol. Struct. **521**, 231 (2000) .
[6] J. Zhang, J. Wang, H. Wang, D. Yana, Appl. Phys. Lett**. 84**, 142 (2004).
[7] P. Peumans, S. R. Forrest, Appl. Phys. Lett. **79**, 126 (2001).
[8] T. Miyata, S. Kawaguchi, M. Ishii, T. Minami, Thin Solid Films **425**, 255 (2003).
[9] S. Antoche, L. Ion, N. Tomozeiu, T. Stoica, E. Barna, Solar Energy Materials and Solar Cells **62**, 207 (2000).
[10] C. Nunes, V. Teixeira, M. Collares-Pereira, A. Monteiro, E. Roman, J. Martin-Gago, Vacuum **67**, 623 (2002).
[11] R. A. Street, J. Graham, Z. D. Popovic, A. Hor, S. Ready, J. Ho**,** Journal of Non-Crystalline Solids **299**, 1240 (2002).
[12] G. Guillaud, J. Simon, J. P. Germain, Coord. Chem. Rev.**178-180**, 1433 (1998).
[13] T. D.Anthopoulos, T. S.Shafai, Appl. Phys. Lett. **82**, 1628 (2003).
[14] M. Kaneko, T. Taneda, T. Tsukagawa, H. Kajii, Y. Ohmori, Japan. J. Appl. Phys. **42**(part1), 2523 (2003).
[15] C. M. Joseph, C. S. Menon, Mater. Lett. **52**, 220 (2002).
[16] W. H.Flora, H. K. Hall, N. R. Armstrong J. Phys. Chem. B **107**, 1142 (2003).
[17] J. Spadavecchia, G. Ciccarella, R. Rella, S. Capone, P. Siciliano, Sensors Actuators B **96**, 489 (2003).
[18] J. S.Shirk, R. G. S. Pong, S. R. Flom, H. Heckmann, M. Hanack, J. Phys. Chem. A **104**, 89 (2000).
[19] L. I. Maissel, R. Glang, Handbook of Thin Film Technology, Mc Graw Hill, NewYork, 1983.
[20] E. A. Ough, J. M. Stillman, Can. J. Chem. **71**, 1891 (1993).
[21] R. A. Collins, A. Krier, A. K. Abass, Thin Solid Films. **229**, 113 (1993).
[22] A. T. Davidson, J. Chem. Phys. **77**, 168 (1982).
[23] J. Bardeen, F. J. Slatt, L. T. Hall, Photoconductivity Conf. 146, Wiley, New York, 1965.
[24] S. Senthilarasu, R. Sathyamoorthy, Cryst. Res. Technol. **41**, 1136 (2006).
[25] Q.Chen, D. Gu, F. Gan, Physica B**. 212**, 189 (1995).
[26] M. E. Azim-Araghi, A. Krier, Pure. Appl. Opt. **6**, 443 (1997).
[27] H. Cao, X. Qiu, Y.Liang, L. Zhang, M. Zhao, Q. Zhu,

Chem. Phys. Chem. **7,** 497 (2006).
[28] S. Im, B. J. Jin, S. Yi, J. Appl. Phys. **87**, 4558 (2000).
[29] F. Gu, S. F. Wang ,M. K. Lu, X. F. Cheng, S . W. Liu, G. J. Zhou, D. Xu, D. R. Yuan, J. Crystal Growth **262**, 182 (2004).
[30] Y. C. Kong, D. P. Yu, B. Zhang, W. Fang, S. Q. Feng, Appl. Phys. Lett**. 78**, 407 (2001).
[31] D. D. Eley, Nature **162**, 819 (1948).
[32] A. Belghachi, R. A. Collins, J. Phys. D: Appl. Phys. **21**, 1647 (1988).
[33] S. Ambily, C. S. Menon, Thin Solid Films **347**, 284 (1999).
[34] M. M. El-Nahass, A. M.Farag, K. F. Abd El-Rahman, A. A. A.Darwish,Opt.Laser Technol. **37**, 513 (2005).
[35] F. Iwatsu, T. Kohayashi, N. Uyeda, J. Phys. Chem. **84**, 3223 (1990).

*Corresponding author: soozan_mathew@yahoo.com